Chapter 7D. A Reevaluation of the Mineral Resources of the Haji-Gak Iron Deposit

By David M. Sutphin, Karine M. Renaud, and Lawrence J. Drew

Abstract

The Haji-Gak iron deposit of eastern Bamyan Province, eastern Afghanistan, was studied extensively and resource calculations made in the 1960s by Afghan and Russian geologists. Recalculation of the resource estimates verifies the original estimates for categories A (in-place resources known in detail), B (in-place resources known in moderate detail), and C_1 (in-place resources estimated on sparse data), totaling 110.8 million metric tons, or about 6 percent of the resources as being supportable for the methods used in the 1960s. C_2 (based on a loose exploration grid with little data) resources are based on one ore grade from one drill hole, and P_2 (prognosis) resources are based on field observations, field measurements, and an ore grade derived from averaging grades from three better sampled ore bodies. C_2 and P_2 resources are 1,659.1 million metric tons or about 94 percent of the total resources in the deposit. The vast P_2 resources have not been drilled or sampled to confirm their extent or quality. The purpose of this report is to independently evaluate the resources of the Haji-Gak iron deposit by using the available geologic and mineral resource information including geologic maps and cross sections, sampling data, and the analog estimating techniques of the 1960s to determine the size and tenor of the deposit.

7D.1 Description of the Deposit

7D.1.1 Location

The Haji-Gak iron deposit in eastern Bamyan Province (fig. 7D–1) is about 100 kilometers (km) west of Kabul in the Turkman Mountains, which may be an extreme western extension of the great Hindu Kush range that exceeds 7,700 meters (m) in elevation in Pakistan (Bouladon and de Lapparent, 1975). The approximate center of the deposit is at latitude 34.683 N. and longitude 68.088 E., but iron mineralization is said to extend discontinuously in an east-west belt over 600 km through central Afghanistan (Afghanistan Geological Survey, undated; Orris and Bliss, 2002; Peters, 2007). The best known and best exposed iron-oxide deposit in Afghanistan, Haji-Gak, forms the crest of Kohe Qarkh, the roughly 3,840-m high peak near the center of the deposit. It can be seen for tens of kilometers when viewed from the south. The focus of this study is the approximately 11-km-long northeast-trending exposure roughly centered at Kohe Qarkh (fig. 7D–2). Close-up images of the Haji-Gak iron deposit are available in Peters and others (2007) and Renaud and others (2011a).

7D.1.2 Exploration

Exploration of the Haji-Gak iron deposit is reportedly extensive (Peters, 2007), but the only available sample data from the deposits came from four drill holes, several trenches and shafts, and an adit (Kusov and others, 1965b). Soviet and Afghan scientists sampled, mapped, and studied the Haji-Gak iron deposit in the mid-1960s and produced geologic maps and resource estimates that after almost 50 years are still the definitive work on the deposit and provide the most often cited resource values

(Kusov and others, 1965b; Orris and Bliss, 2002; Peters, 2007). Most of this summary is a translation of that nearly 50-year-old work that was completed before many modern concepts of ore genesis, plate tectonics, and radiometric age dating became commonplace.

Figure 7D–1. Panoramic view of part of the Haji-Gak iron deposit as seen from the southeast. (Original photographs by Jeff Doebrich, U.S. Geological Survey, 2006)

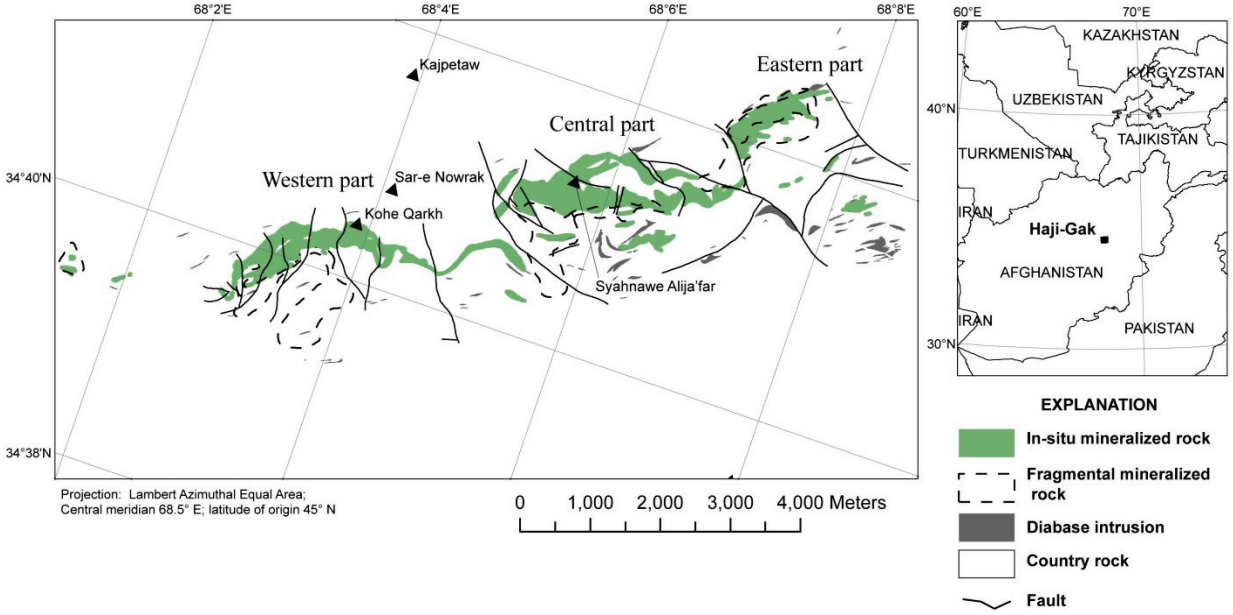

Figure 7D–2. Map of the Haji-Gak iron deposit in Eastern Afghanistan (after Renaud and others, 2011a,b).

Geochemical stream-sediment exploration was done throughout the Haji-Gak area (Peters, 2007). In 1972, a Franco-German group made a feasibility study on the deposit. This study suggested the construction of a blast furnace near the deposit, as coking coal is available from the nearby Dar-i-Suf district (Afghanistan Geological Survey, undated). Afghan, German, French, and Russian feasibility studies made on the deposit also have been completed (Afghanistan Geological and Mineral Survey, 1967; DEMAG, 1974; Venot-Pic, 1974). In early 2011 it was speculated that a mining company would build a railroad to transport raw ore northward out of Afghanistan (U.S. Departments of State and Defense, 2011). Other iron occurrences have not been extensively explored as Haji-Gak.

In 2006, a U.S. Geological Survey (USGS) assessment team visited the area briefly, took photographs, and collected grab samples (Peters, 2007; Jeff Doebrich, February 2, 2006, written commun.). A flurry of intense interest in Haji-Gak is expected in 2011 and beyond, despite security concerns, because the Islamic Republic of Afghanistan has invited 22 companies from such countries as

Canada, China, India, and the United Kingdom to bid for the right to mine iron at the deposit (Robinson and Shalizi, 2011).

7D.1.3 Geology

Kusov and others (1965b) detailed the geology of the Haji-Gak iron deposit and the surrounding area, and the British Geological Survey and the Afghanistan Geological Survey have updated the stratigraphic nomenclature (Afghanistan Geological Survey, undated). The Haji-Gak deposit is part of the iron-mineralized zone that occurs discontinuously in a 600-km-long east-west belt from Herat to the Panjsher River. At Haji-Gak, the iron mineralization[1] occurs within the Herat fault-zone in subconcordant sheets and lenses within Proterozoic metasedimentary and metavolcanic rocks (Afghanistan Geological Survey, undated).

7D.1.3.1 Stratigraphy at the Haji-Gak Deposit

The basement rocks of the Haji-Gak deposit are the Mesoproterozoic Jawkol Formation, which consists of gray silicified limestones and dolomites (probably marbles) interbedded with dark-gray crystalline schists and light-colored quartzites metamorphosed to amphibolite facies (Afghanistan Geological Survey, undated). The Neoproterozoic Kab Formation unconformably overlies the Jawkol Formation, which consists of dark-gray sericitic schists, interpreted as metamorphosed terrigenous sedimentary rocks, felsic volcanic rocks, minor marbles and phyllites, and lenses of altered volcanic rocks (Kusov and others, 1965b; Afghanistan Geological Survey, undated). Figure 7D–3 shows the stratigraphy at the Haji-Gak iron deposit.

Neoproterozoic rocks of the Awband Formation were deposited conformably on the Kab Formation. The Awband Formation consists of schists, dolomitic and calcitic marbles, and sericitic quartzites containing interbeds of volcanic rocks. These rocks have been metamorphosed to greenschist facies. The Haji-Gak iron deposit consists of a series of folded and faulted iron-rich lenses. The lenses have been altered and contain cross-cutting iron veins. The iron-bearing rocks have been widely seritized and silicified (Kusov and others, 1965b). The Neoproterozoic Green Schist Formation was deposited conformably on the Awband Formation. It consists of greenschists (metamorphosed volcanic tuffs) (Afghanistan Geological Survey, undated).

Upper Devonian sedimentary rocks of the Haji-Gak Formation disconformably overlie the Green Schist Formation. The Haji-Gak Formation consists of limestones, conglomerates, sandstones, and pelitic schists containing a fauna of Upper Devonian brachiopods and corals (Kusov and others, 1965b). It is faulted against the Green Schist Formation (Afghanistan Geological Survey, undated). Resting on the Haji-Gak Formation are the sedimentary rocks of the Upper Carboniferous Horzar Formation, a sequence of pelitic schists, quartz-rich schists, sandstones, quartzites, and conglomerates. In the southwest part of the area, Lower Cretaceous and younger cover rocks lie unconformably on the older rocks. The lower section of the Lower Cretaceous rocks consists of red conglomerates, sandstones, and limestones. The Neogene rocks are gently dipping beds of red conglomerates and sandstones (Kusov and others, 1965b). The uppermost of these younger deposits are, in part, the talus or scree deposits of fragmental iron-mineralized rocks that has been eroded from the in-situ iron deposit.

---

[1]In the 1960s study of the Haji-Gak deposits, Kusov and others (1965b) used the term "ore" to define any rock that was thought to have iron mineralization. In that study, "ore blocks" were located in "ore bodies," and "ore" was designated as in A, B, C_1, C_2, fragmental, and P_2 "ore categories." In this paper on the same deposit, the term "ore" is restricted to material containing iron mineralization in sufficient quantity and grade and chemical combination as to make extraction commercially profitable (Thrush and others, 1968). Instead of "ore," the terms "mineralized material," "mineralized rock," and "resources" are used.

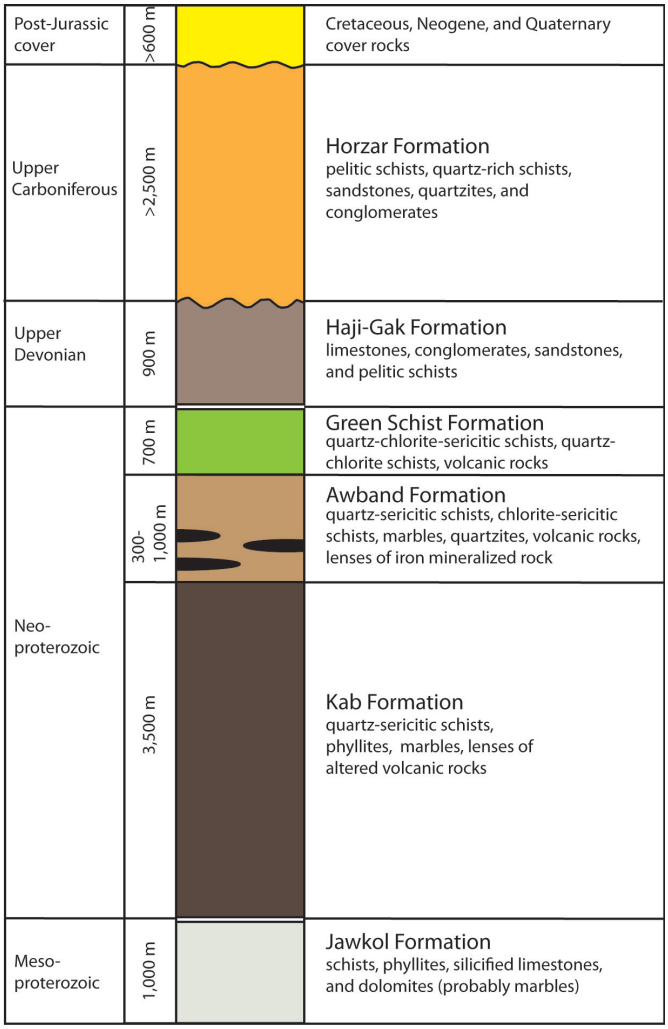

Figure 7D–3. Stratigraphy at the Haji-Gak iron deposit, central Afghanistan (Afghanistan Geological Survey, undated; as modified from Kusov and others, 1965b).

7D.1.3.2 Plutonic Rocks

The area of the Haji-Gak iron deposit is known for its complex magmatic activity that extended over a long time period and includes both plutonic and volcanic rocks. The volcanic rocks are briefly covered in the descriptions of the stratigraphy.

Kusov and others (1965b) divided the plutonic rocks into five types; 1) serpentine, that occurs in thin (up to 5 m) dikes and sills in the Jawkol Formation and consists of green schistose fine-grained rocks; 2) diabases that occur as hypabyssal intrusions up to 1 km in diameter and are commonly found among the Paleozoic rocks in the region. Kusov and others (1965b) suggests that the diabases and serpentines were emplaced starting sometime after the Early Carboniferous and before the end of the Triassic or the beginning of the Jurassic as mafic and ultramafic magmatism ended and granitic magmatism began. 3) Granitic plutons are common in the region where they cut Upper Triassic deposits and are overlain by Middle Jurassic deposits. 4) Small granitoids occur in small massifs and stocks of plagiogranites, granodiorites, quartz diorites, and quartz diorite porphyries as much as 600 m wide by 2,000 m long. The granites and the small granitoid plutons may have had the same source as the granitoid magmatic complex (Kusov and others, 1965b). 5) The last plutonic rock type, alkaline rocks, occurs as sparse thin dikes and veins of keratophyres and stock-like bodies of metasomatic carbonatites as much as 300 m in diameter. They appear to have been emplaced somewhat later or simultaneously with the small granitoids.

7D.1.4 Structural Geology

The structural geology of the Haji-Gak deposit is described in detail in Kusov and others (1965b) and summarized in chapter 7A of this report. This section is condensed from those works.

The rocks of the Haji-Gak iron deposit form a large monocline, which coincides with the south limb of a larger anticlinorium. The monocline in turn contains smaller folds and fractures. The mineralized bodies are conformable with the host rocks and with the folded structure of the entire region. The rocks in the deposit strike northeast and dip steeply to the southeast.

The eastern part of the deposit contains small-scale isoclinal, locally recumbent, folds. Faults in the eastern part are brittle. The central part of the deposit consists of the Awband and Green Schist Formations and is composed of rocks, such as iron minerals, schists, quartzite, marble, and volcanic rocks and alkaline plutonic rocks, which have contrasting physical characteristics. That contrast played a major role in the intense faulting and folding seen in this section. There are small symmetric and asymmetric folds, often overturned and recumbent. The schists are kink-banded. The bodies of iron mineralization are fractured parallel to cleavage. Banded mineralized material in the deposit is sheared and marked by cleavage parallel to the schistosity. In the western part of the deposit the rocks are deformed, especially near faults, but not as much as those rocks in the central part. The carbonate rocks of the western part are fractured and contain horse-tail fractures.

Faults in the Haji-Gak area are transverse, diagonal, and occasionally parallel to the bedding and schistosity. The faults vary from large to small, and consist of strike-slip dip-slip faults, thrust faults, normal faults, and shear faults along cleavage. Normal faults are present in the mineralized bodies and on the contacts between the bodies and host rocks. The displacement varies from 1 to a few meters and in places as much as 10 m. These faults usually are splays from the larger faults.

In general, Kusov and others (1965b) recognized that the Haji-Gak iron deposit has been folded and is confined to the limb of a monocline, which was refolded and fractured. An early period of folding was interpreted by Kusov and others (1965b) to have occurred at the end of the Triassic and the beginning of the Jurassic during the Cimmerian Orogeny. Another period of folding probably occurred in the Paleogene during the Alpine Orogeny, and the area is tectonically active today (Kusov and others, 1965b).

7D.1.4.1 Mineralized Rock

Kusov and others (1965b) identified 16 bodies (1–16) of in-situ iron mineralization and 4 bodies (A–D) of fragmental mineralized scree material at Haji-Gak. Of the 16 in-situ mineralized bodies, 7 are in the western part of the deposit, 6 in the central part, and 3 in the eastern part of the deposit. The A and B fragmental bodies are in the western part of the deposit; the C fragmental body is in the central part of the deposit, and the D fragmental body is in the eastern part of the deposit. Figures 7D–4 through 7D–6 show the mineralized bodies in their respective parts of the Haji-Gak iron deposit.

Kusov and others (1965b) described the in-place original (nonfragmental) mineralized material as being confined to the Awband Formation, which is up to 1,200 m thick and about 12 km in length along strike. The Haji-Gak iron deposit crops out along the southern slopes of the mountains as rocky ridges along the northeast-southwest trend of the ridge crest (figure 7D–1). The mineralized bodies are further exposed where valleys have cut the deposits. The bodies occur as tabular or lenticular masses whose strike and dip coincide with the predominant folded structure of the region. The mineralized bodies are confined to the southern limb of a regional anticlinorium. These bodies at places have been broken by postmineralization faults and occur in individual blocks. The mineralized material is secondarily zoned and sheared. Mineralized material as much as 100 to 130 m below the present surface is partly oxidized or oxidized. The non-oxidized material is made up of magnetite (40–90 percent) and pyrite (2–35 percent). Partly oxidized material is divided into three types: hydrogoethite-half-martite, hydrogoethite-hematite-half-martite, and carbonate-half-martite. Around the Haji-Gak iron deposit, the country rocks have been silicified, sericitized, chloritized, and locally carbonatized. Near the

mineralized bodies, the schists are silicified and in places converted into banded sericitic quartzites. Schists formed from felsic tuffs are mostly sericitized, whereas those formed from mafic tuffs are chloritized and carbonatized. Dolomites (probably marbles) are silicified (Kusov and others, 1965b).

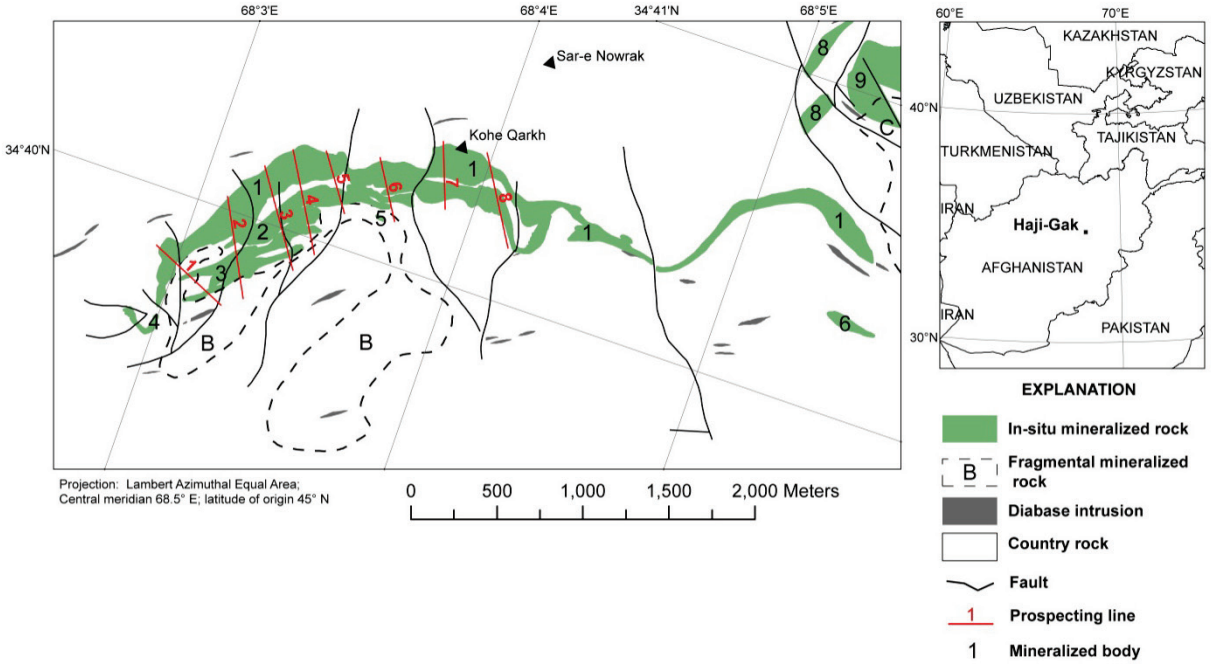

Figure 7D–4. Locations of in-situ iron mineralized bodies, fragmental bodies, and prospecting lines in the western part of the Haji-Gak iron deposit (after Renaud and others, 2011a, b). Small in-situ iron-mineralized body 7 and fragmental body A, located farther to the west, are not shown.

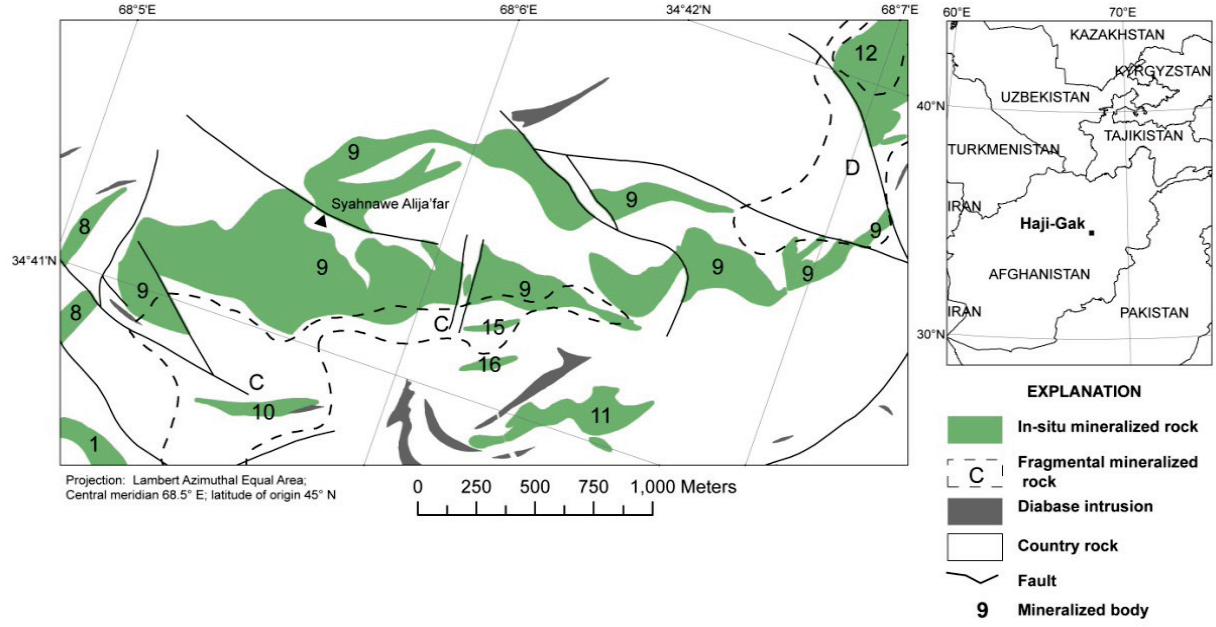

Figure 7D–5. Locations of in-situ iron mineralized bodies and fragmental bodies in the central part of the Haji-Gak iron deposit (after Renaud and others, 2011a, b).

7D.1.4.2 Fragmental Ores

Fragmental mineralized bodies are alluvial-talus slope deposits of iron-rich material weathered from the original in-situ Haji-Gak iron deposits. They are of limited thickness but cover considerable areas at the base of the outcrops of the in-situ iron deposits and spread down slope for as much as 1.5 km. The reported area of the deposits ranges from 100,000 m^2 to 859,690 m^2, and thickness ranges from 1.9 to 17.0 m with an average of about 6.75 m (Kusov and others, 1965b).

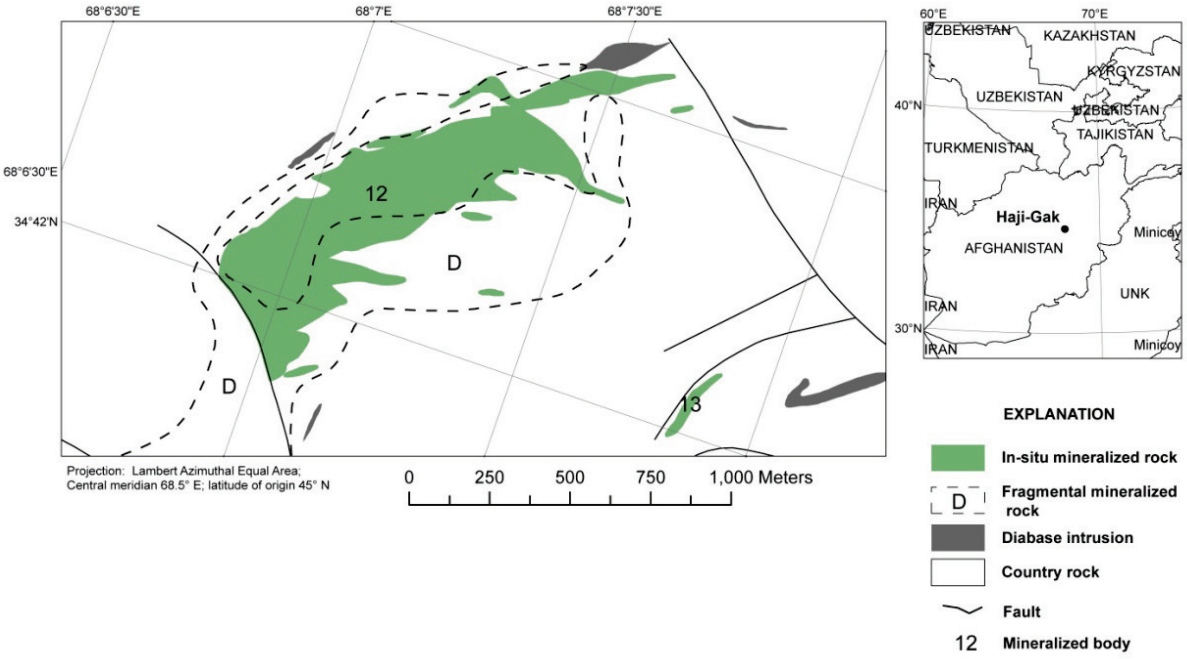

Figure 7D–6. Locations of in-situ iron-mineralized bodies 12 and 13 and fragmental body D in the eastern part of the Haji-Gak iron deposit (after Renaud and others, 2011a, b). In-situ iron mineralized body 14, located to the southeast of mineralized body 13, is not shown.

7D.1.5 Origin of the Haji-Gak Iron Deposit

De Lapparent (1961) concluded that the Haji-Gak iron deposit was formed by the leaching of silicic ferrous iron formation producing a secondary concentration of hematite in favorable horizons. In contrast, Brueckl (1935) concluded that the Haji-Gak deposit formed by contact metasomatism.

Kusov and others (1965b), based on extensive field examination of much of the Haji-Gak iron deposit, proposed that it had formed at moderate to considerable depth during Early Jurassic tectonic-magmatic activity. In this scenario, mineralization occurred in three phases: (1) dolomitization and silicification of the country rocks and deposition of magnetite, hematite, and quartz; (2) carbonization and seritization of the country rocks with deposition of hematite, pyrite, and quartz with siderite and barite; and (3) superposed pronounced veins, veinlets, and impregnations of siderite and rare pyrite with quartz, and barite carbonates (Kusov and others, 1965b).

Bouladon and de Lapparent (1975) recognized that mafic lavas and tuffs, converted to greenschists, always occurred near the mineralized bodies at Haji-Gak. They proposed that the Haji-Gak iron deposit resulted from submarine-exhalative processes synchronous with mafic volcanic activity in a succession of events. First, a sedimentary basin with andesitic submarine volcanism formed tuffs, lava flows, and sericitic and chloritic sediments of exhalative origin. At the same time, hematite and magnetite precipitated from mixing of the hydrothermal fluids. This could have been in a seafloor environment where ancient “black smokers” vented hot mineral-laden waters. Later, gabbro and diabase sills were

intruded, which resulted in iron oxides being remobilized into fractures across gabbro boundaries and replacing neighboring dolomites (Bouladon and de Lapparent, 1975). Lastly, rocks of the Haji-Gak area were affected by two major kinds of metamorphism: firstly, of greenschist facies, contemporaneous with intrusive activity; secondly, mainly east of Haji-Gak, sericitic dynamometamorphism, during folding.

Peters (2007) reported four metallurgical types of mineralized material: hydrogoethite-polymartite, hematite-polymartite, carbonate-polymartite, and hydrogoethite-polymartite; the latter has the highest iron grade. Metallurgically deleterious elements are sulfur in the form of sulfate (0.04 to <5 percent S, and phosphorus (7 lump samples ranged from 0.0 to 0.28 percent P_2O_5 (Kusov and others, 1965b; Peters, 2007). Pyrite-magnetite mineralization (magnetite 40–90 percent and pyrite 2–35 percent) is rich in iron, averaging 61.30 percent iron, but the sulfur content averages 4.56 percent (Kusov and others, 1965b). Questions still exist as to the timing of the chemical weathering that oxidized part of the magnetite mineralization to hematite with lesser martite at Haji-Gak (Abdullah and others, 1977; Orris and Bliss, 2002). The mineralization at Haji-Gak is described as being massive, rather than interlayered, with iron-poor shale and bands of chert as are commonly found in sedimentary iron deposits. Renaud and others (2011a,b) show that a sample from Haji-Gak has banding with primary textures that likely formed in a sedimentary setting.

7D.1.5.1 Geologic Age

The geologic age of the Haji-Gak iron deposit is not known with certainty. The modern interpretation shown in figure 7D–3 is that it is Neoproterozoic (Afghanistan Geological Survey, undated). However, in their massive work on the deposit, Kusov and others (1965b) suggested that the sequence of sedimentary and volcanic rocks that form the Awband Formation, where the iron mineralization at Haji-Gak occurs, was deposited in the early to middle Paleozoic (possibly Late Ordovician), on the basis of poorly preserved corals. Subsequently, Bouladon and de Lapparent (1975) proposed that the Haji-Gak iron deposit formed during the early Paleozoic, maybe Silurian to Lower Devonian based on its stratigraphic position in the Awband Formation above metamorphosed Proterozoic gneiss and below beds containing Late Devonian fossils.

7D.1.5.2 Mineral Deposit Type of the Haji-Gak Iron Deposit

Geologists use mineral deposit models to compare their observations with the collective knowledge and experience of a much wider group of geoscientists (Cox and others, 1986). Once a deposit is determined to fit a certain mineral deposit model, its similarity to and difference from the model can be discussed in terms of its genesis and other characteristics.

In the Peters and others (2007), the Haji-Gak iron deposit is not classified as to its specific mineral deposit type, because the U.S. Geological Survey mineral-resource specialist he consulted said that he could not provide "enough information on the [deposit] to determine which (if any) deposit model best described it." That situation has not changed. At present, there is not enough detailed reliable, first-hand information available on the geology of Haji-Gak iron deposit to make a confident determination of which mineral deposit model it best fits. Only when better access to the deposit is secured and scientists can study and sample Haji-Gak with modern techniques will the deposit model that best describes Haji-Gak be determined.

7D.1.6 Haji-Gak Iron Deposit in Google Earth

The Haji-Gak iron deposit can be seen clearly in images in Google Earth. It looks much as it does in published aerial images (Renaud and others, 2011a). That is, it appears as dark cliffs on the crests of a series of mountains (fig. 7D–7). The slopes are steep and the crests of the mountains form very narrow ridges. The three naturally divided parts of the deposit, western, central, and eastern, are identified by the intermittent patches of iron mineralization. The deposit consists of several roughly 1-km-long

patches of black to dark-brown cliff faces and talus slopes where the iron deposit is exposed on the surface. There appear to be pods of iron mineralization near the mountain peaks with dark mottled areas where the iron-rich talus (fragmental mineralization) trails down the east side of the mountains (fig. 7D–7). When seen in Google Earth or in outcrop, it is easy to understand the enthusiasm for Haji-Gak as a potentially large iron mineral resource.

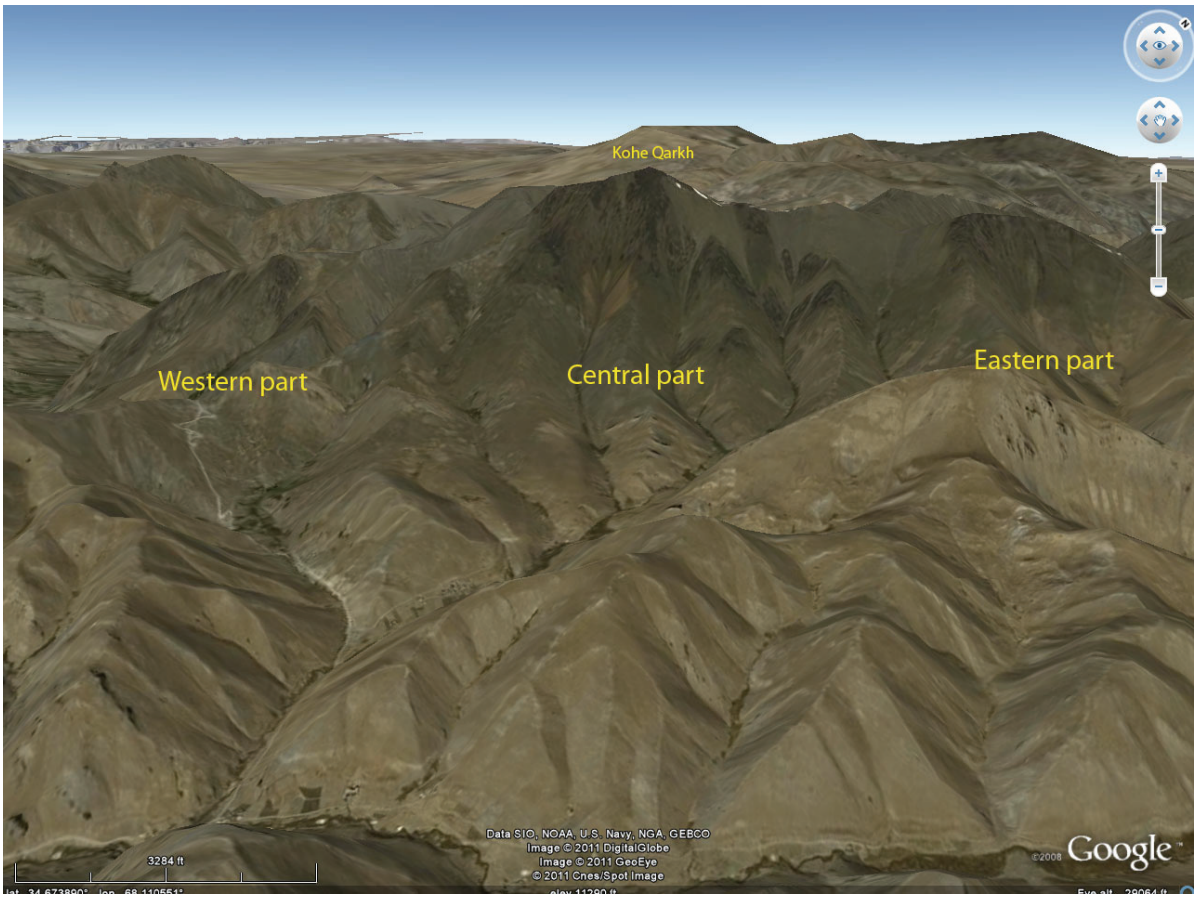

Figure 7D–7. Location of the three parts of the Haji-Gak iron deposit as seen from the southwest in Google Earth.

7D.2 Reported Resources

According to previous reports, Haji-Gak has been described as a world-class iron deposit with enormous mining potential (InfoMine, 2011). A look through the recent press finds reports of resources of 1.8 billion tons of iron "ore," having a grade of approximately 62 percent iron, that is "truly significant on a global scale" (Afghanistan Ministry of Mines, 2011; InfoMine, 2011); and "the Ministry estimates the worth of its reserves at as much as $350-billion" (Mining Weekly, 2011).

A major purpose of this paper is to evaluate how the resource figures were derived and to assess their validity. Table 7D–1 is a listing of the published resource figures for the Haji-Gak iron deposit.

7D.2.1 Definitions of Resource Categories

The Soviet system divides mineral occurrences into seven categories, which fall into three major groups based on the level of exploration received: fully explored resources (categories A, B, and C_1), evaluated resources (category C_2), and prognostic resources (categories P_1, P_2, and P_3) (Henley, 2004). The prospective mineral deposits are explored by drill holes, shafts, and trenches arranged in lines

perpendicular to the strike of the deposit. These explorations form prospecting lines along which samples of mineralization are collected and measurements are recorded. To make the resource estimates, the deposits are conceptually divided into mineralized bodies, which are in turn divided into mineralized blocks that extend between a series of vertical planes along the prospecting lines (fig. 7D–4; Kužvart and Böhmer, 1978). Profiles of the mineralized bodies are drawn along the prospecting lines, areas of the mineralized bodies are calculated where they intersect the prospecting lines, and the volumes of the mineralized bodies and their tonnages of resources are calculated between the prospecting lines.

Table 7D–1. Iron resources at the Haji-Gak iron deposit identified following Afghan-Soviet exploration in the 1960s.

[Data are from Kusov and others (1965b) and Afghanistan Geological Survey (undated). n.a., not applicable]

Soviet resource category	Equivalent classification	Material type	Quantity (million metric tons)	Percentage of total material	Iron (percent)	Sulfur (percent)
A	Measured or proved (highly detailed)	Oxidized	9.1	0.51	62.52	0.14
B	Measured or proved (moderate detail)	Oxidized	19.2	1.08	62.69	0.09
C_1	Indicated or probable	Oxidized	65.1	3.68	62.15	0.13
C_1	Indicated or probable	Primary	16.2	0.92	61.3	4.56
C_1	Indicated or probable	Fragmental	1.2	0.07	60.62	0.08
C_2	Inferred or possible reserves	All types	314.3	17.76	n.a.	n.a.
C_2	Inferred or possible reserves	Fragmental	2.9	0.16	n.a.	n.a.
P_2	Reconnaissance resources	All types	1,333.30	75.33	n.a.	n.a.
P_2	Reconnaissance resources	Fragmental	8.6	0.49	n.a.	n.a.
		Total	1,769.90	100.00	n.a.	n.a.

7D.2.1.1 Fully Explored Resources

Category A.—These are areas where the in-place resources are known in detail. The boundaries of the deposit have been outlined by trenching, drilling, and underground workings (Henley, 2004). This material meets the highest grade and tonnage standards with a minimum of deleterious materials, and is easily worked.

At Haji-Gak, category A resources have been explored and sampled by trenches, drill holes, shafts, and an adit. Two blocks, 3A and 4A, in mineralized body 1 meet these standards (fig. 7D–8). Table 7D–2 lists the resource blocks by the mineralized body in which they are located and by resource category (after Kusov and others, 1965b).

Category B.—These resources are in-place and have been explored but are known only in moderate detail. The boundaries of the deposit have been outlined by trenching, drilling, or underground workings. The quality and properties of the mineralized material are known in sufficient detail to ensure the basic reliability of the exploitation (Henley, 2004).

At Haji-Gak, resource blocks 2B, 5B, and 6B in mineralized body 1 have been explored in detail enough to fall into category B (fig. 7D–8).

Category C1.—These are areas where the in-place resources have been estimated by a sparse grid of trenches, drill holes, and underground workings. This category includes resources adjoining A and B resources and resources in very complex deposits where even a dense grid cannot determine the resources adequately (Henley, 2004).

At Haji-Gak, C_1 resources are exposed adjacent to and beneath the A and B resource blocks in mineralized body 1 (fig. 7D–8) and exposed in mineralized body 2 (fig. 7D–9). Several of the mineralized blocks at Haji-Gak have their C_1 resources divided into C_{1a} and C_{1b} resources based on the conditions and extent of exploration. Estimates of C_{1a} resources are made using drill holes as the

principal source of sample data, while C_{1b} resources rely on a combination of drill holes and underground workings for samples (Kužvart and Böhmer, 1978).

Table 7D–2. Locations of resource blocks by mineralized body and category.

[Data are from Kusov and others (1965b). All resources not in categories A, B, C1, or C2 in any mineralized body are included in the P2 category. Fragmental body A is too small to be evaluated]

Ore body	Resource blocks by category				
	A	B	C_1	C_2	P_2
1	3, 4	2, 5, 6	1, 7, 8, 9	10, 11, 12	✓
2	—	—	13, 14	15, 16, 17, 18	✓
3–8	—	—	—	—	✓
9	—	—	—	20, 21, 22, 23	✓
10–16	—	—	—	—	✓
Fragmental mineralization bodies					
B	—	—	—	—	✓
C	—	—	—	—	✓
D	—	—	—	—	✓

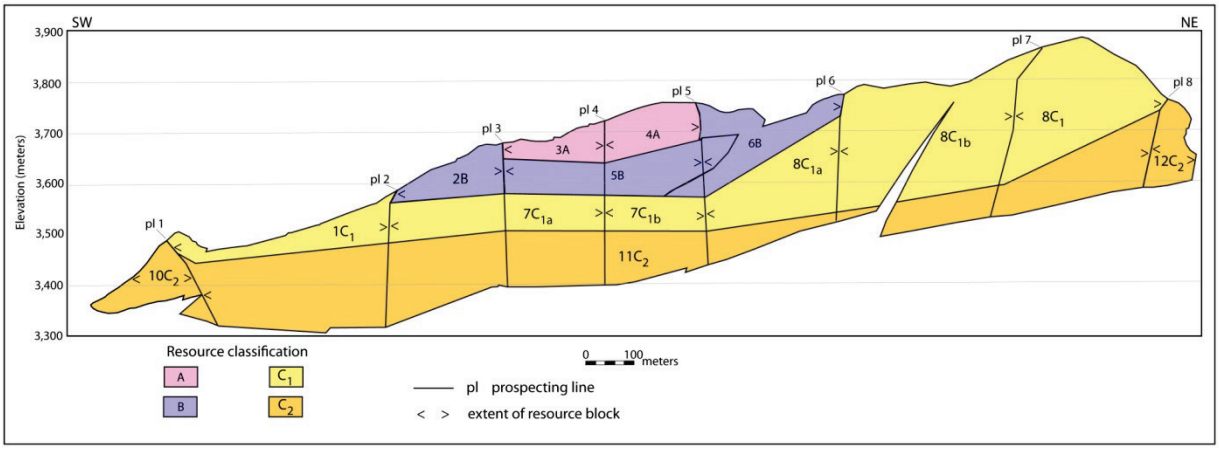

Figure 7D–8. Vertical longitudinal projection of mineralized body 1 (see figure 7D–4) showing the prospecting lines, and the resource blocks within the body (after Kusov and others, 1965b).

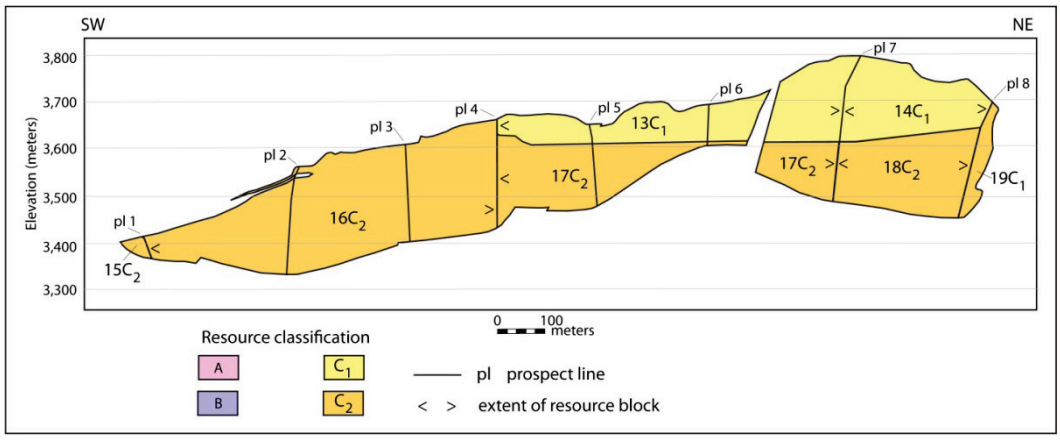

Figure 7D–9. Vertical longitudinal projection of mineralized body 2 (see figure 7D–4) showing the prospecting lines, and the resource blocks within the body (after Kusov and others, 1965b).

7D.2.1.2 Evaluated Resources

Category C2.—C_2 resources are based on a loose exploration grid with little data (Henley, 2004). The limits of the mineralization were determined by extrapolation of the identified geological structures and from comparison with nearby deposits. C_2 resources include resources that are adjacent to A, B, and C_1 resources in the same deposit (Henley, 2004).

C_2 resources at Haji-Gak are located in mineralized bodies 1, 2, and 9, the bodies that were explored to the extent that fully explored or evaluated resources were defined (figures 7D–8, 7D–9, and 7D–10).

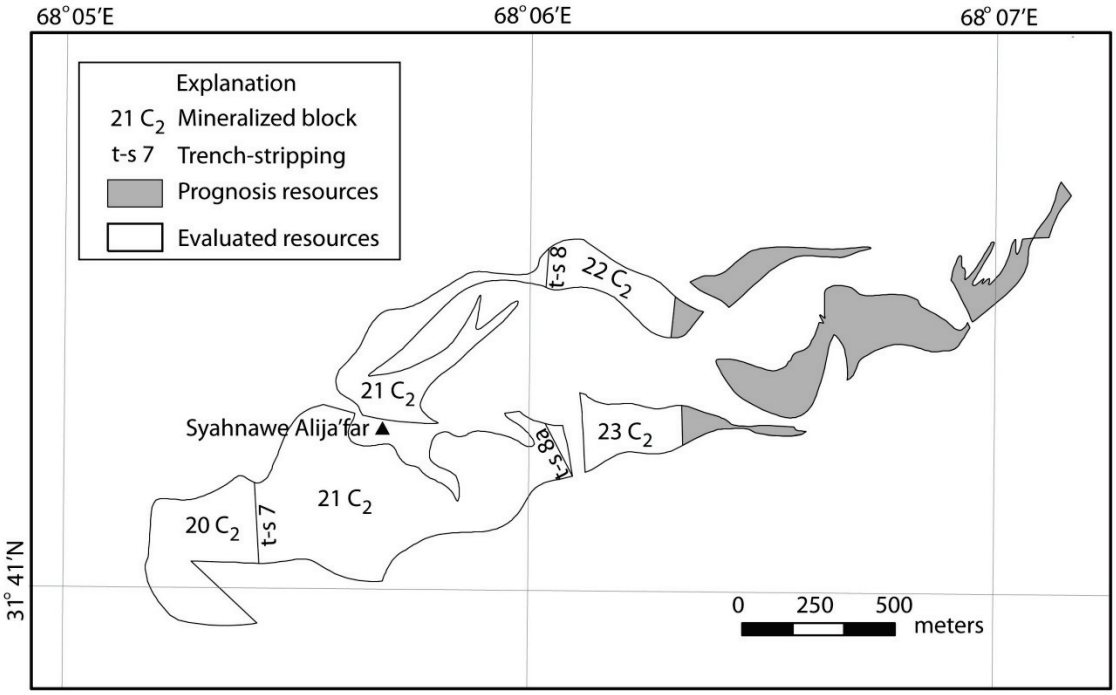

Figure 7D–10. Map view of resource blocks and prognosis material of mineralized body 9 (after Kusov and others, 1965b).

7D.2.1.3 Prognostic (Prognosis) Resources

Prognosis resources are those that are estimated for mineralized rock outside the actual limits of areas that have been explored in detail and are commonly based on data from trenches and from geochemical and geophysical surveys (Henley, 2004). Henley (2000) suggests that prognosis resources "are largely wishful thinking and have no equivalent" in western classifications.

Category P1— Indirectly estimated resources that may extend beyond the limits of C_2 resources.

There are no P_1 resources identified at Haji-Gak by Kusov and others (1965b).

Category P2—These are prognosis resources that represent possible mineral structures in known mineral deposits in mineralized regions (Henley, 2004). They are usually based on geochemical and geophysical data. Shape, mineral composition, and size of the area of mineralization are estimated by analogy with similar mineral occurrences in the area.

All of the known mineralized bodies at Haji-Gak, both in-situ and fragmental mineralization, have estimated P_2 resources. These resources are roughly calculated and characterize the potential possibilities of the Haji-Gak deposit (Kusov and others, 1965b). P_2 resources account for 93.74 percent of the mineralized material at Haji-Gak.

Category P3—These are any remaining resources not in other categories. Kusov and others (1965b) identified no P_3 resources at Haji-Gak. As mapped and studied by Kusov and others (1965b), the 16 separate mineralized zones in the Haji-Gak iron deposit are as much as 5 km long, 380 m wide, and

extend as much as 550 m down dip (Kusov and others, 1965b; Peters, 2007). Three mineralized zones, numbers 1, 2, and 9, were studied in greater detail than the others by Kusov and others (1965b).

Two types of mineralization, primary and oxidized, have been identified. Kusov and others (1965b) speculated that primary mineralization, which makes up about 80 percent of the resource estimate, occurs below a depth of about 100 to130 m and consists of magnetite (40–90 percent) and pyrite (2–35 percent) with minor other sulfides including chalcopyrite (single grains). Primary mineralization averages 61.3 percent Fe, 5 percent sulfide, and 0.05 percent P. The remaining 20 percent of the deposit is oxidized material that consists of three hematitic mineralization types and contains about 62.8 percent Fe. Soviet-Afghan estimates for the entire deposit are 1,769.9 Mt, although estimates for the near-surface oxide ore in the most explored area are 85 Mt (Categories A–C_2) (Afghanistan Geological Survey, undated; Momji and Chaikin, 1960; Kusov and others, 1965a, b; Bouladon and de Lapparent, 1975; Abdullah and others, 1977; *http://www.bgs.ac.uk/afghanminerals/femetals.htm*). A compilation by the U.S. Geological Survey cited the indicated resources as 100 Mt at 61.3 percent Fe and inferred resources as 2,070 Mt at 62.83–68.68 percent Fe (table 7D–3) (Orris and Bliss, 2002).

7D.2.2 Review of Haji-Gak Resource Calculations

Exploration of the Haji-Gak deposit was done in 1963 and 1964 by as many as 220 workers from the Geological and Mineral Survey Department of the Ministry of Mines of the Royal Government of Afghanistan with technical assistance from the Soviet Union (Kusov and others, 1965b). That exploration produced a series of estimates of the iron resources at Haji-Gak calculated from field measurements and observations. The purpose of resource calculations of a mineralized body is to determine the quantity, quality, and amenability to commercial exploitation of the mineralized raw material. These calculations are made at every stage of a deposit's life from discovery to mining to closing (Popoff, 1966). Efficient extraction and production is impossible without accurate resource calculations.

The Soviet resource reporting system was different in principle and detail from the principal reporting codes used by other nations (Henley, 2004). The former Soviet system for classification of reserves and resources was developed in 1960, revised in 1981, and is still used today in Russia and other former CIS republics (Henley, 2004). Conditions pertaining to classifying the iron resources at Haji-Gak are listed in Kusov and others (1965b). The resource categories are described in Kužvart and Böhmer (1978) and Henley (2004).

A review of the Soviet-era methodology and grade and tonnage resource calculations as described by Kusov and others (1965b) and explained by Popoff (1966) and Henley (2004) is appropriate to understand their methodology and to verify their assumptions and calculations.

7D.2.2.1 Profiles of the Mineralized Bodies

In the 1960s when the Soviet-Afghan exploration was being done, profiles of the identified mineralized bodies were drawn to show the prospecting lines, trenches, an adit, and drill holes. The profiles were used to aid the explorationists to visualize the deposit and to determine how to best calculate its mineral resources. Figures 7D–8 and 7D–9 show simplified profiles of mineralized bodies 1 and 2 (Kusov and others, 1965b).

Table 7D–3. Information about the Haji-Gak iron deposit.

[Data are from Orris and Bliss (2002)]

Type of deposit	Host rock age	Host rock	Significant minerals or materials	Deposit size and (or) grade	Comments	References
Volcanosedimentary, hydrothermal-metasomatic	Proterozoic	Ferruginous quartzite	Hematite, magnetite, martite, hematite, siderite, pyrite	Indicated—100 Mt grading 61.3% Fe Inferred—2,070 Mt grading 62.83–68.68% Fe	The largest iron deposit in the Middle East and extends over 600 km. There are primary and semioxidized ores. At least 16 ore bodies; most are small.	ESCAP, 1995; Chmyriov and others, 1973; Abdullah and others, 1977; Afzali, 1981

7D.2.2.2 Soviet Methodology for Estimating Areas

The methodology that the Soviet-Afghan exploration party of 1963–64 used for measuring and estimating iron resources of the Haji-Gak deposit included mapping the deposit at a regional scale of 1:50,000 and locally in detail at 1:10,000. In the western part of the deposit, exploratory holes were drilled and shafts were sunk into the mineralized rock, trenches were dug across the deposit, samples were taken, and cross sections were drawn to show in profile view the vertical slices through the deposit along traverses (prospecting lines) at various intervals (Kusov and others, 1965b). Information from the prospecting lines, drill holes, and trenches was used to create the cross sections. The western part of the deposit has category A and B resources commensurate with this level of exploration. The central and eastern parts of the deposit were much less well explored and have resource categories reflecting a lesser certainty of the resources. Figure 7D–11 shows a cross section along prospecting line 1 (see fig. 7D–4; Kusov and others, 1965b).

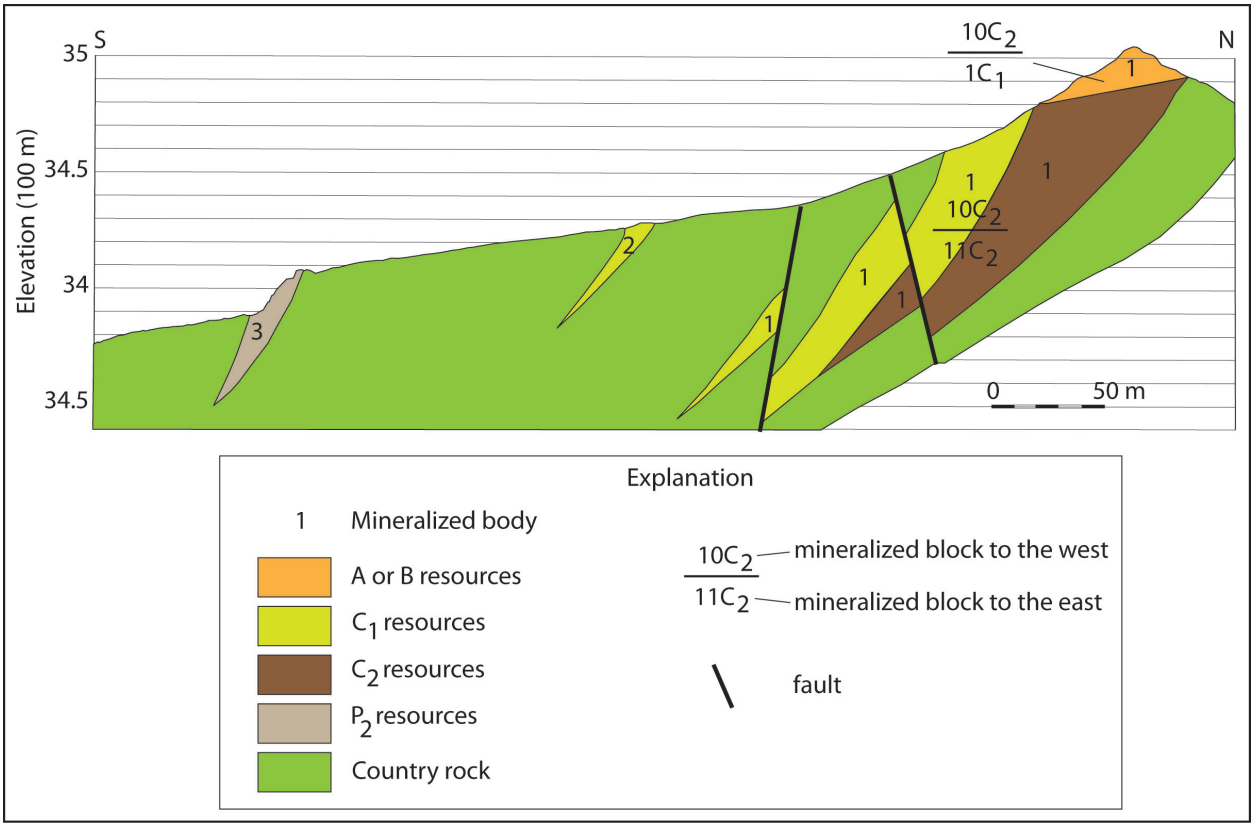

Figure 7D–11. Cross section along prospecting line 1 of the Haji-Gak iron deposit crossing mineralized bodies 1, 2, and 3 (fig. 7D–4.)

As explained in Kusov and others (1965b), for resource categories A, B, C_1, and C_2, the cross sections were drawn at a scale of 1:1,000 so that the area of each resource block where it intersected prospecting line could be estimated by simply drawing 5 mm x 5 mm squares on the cross section (fig. 7D–11), counting the number of squares in the cross section of a particular resource block, and multiplying the number of squares by 25 m^2, the area represented by each 5 mm x 5 mm square at a scale of 1:1,000. These cross-sectional areas were used as the areas of ends of solid geometrical figures, such as cones, frustums, and wedges, which were selected to best represent the shapes of the mapped resource blocks. The volume computations were made by substituting graphically the irregular shape of the mineralized body with imaginary simple solid geometric figures (Popoff, 1966). Using the

geometrical figures, their cross-sectional areas, the measured distances between the prospecting lines along which the cross sections were drawn, and the appropriate formulas for finding the volumes of simple solid geometrical figures, the volumes of resources in each mineralized block were calculated (Kusov and others, 1965b; Popoff, 1966). Figure 7D–12 shows common geometric shapes used for resource calculations, figure 7D–13 shows the upper part of mineralized body 1 of the Haji-Gak iron deposit as represented by solid geometrical figures used in calculating the amount of resources, and tables 7D–4A, B, and C show the dimensions of the mineralized blocks, the geometric shapes used to represent the mineralized blocks, the volume of the blocks, and the amount of mineralized material in each mineralized block estimated in the Haji-Gak iron deposit.

7D.2.2.3 Calculating the Iron Resources in Mineralized Body 1

The information in tables 7D–4A, B, C was used to calculate the estimated amount of iron-mineralized material in all of the designated mineral blocks for categories A, B, C_1, and C_2 at Haji-Gak. For example, the first row of data in table 7D–4A shows that block 3A is located between cross sections 3 and 4. Block 3A has an area equal to 72 25-m^2 squares or 1,800 m^2 in cross section 3 and an area of 345 25-m^2 squares or 8,625 m^2 in cross section 4. The unequal areas of the ends suggest that the geometric shape to best represent block 3A is a frustum, which table 7D–4A shows. The distance between cross sections 3 and 4 is listed in table 7D–4A as 202 m. The formula given in the table to calculate the volume of a frustum is:

$$V= L*((S_1+S_2 + sqrt\ (S_1*S_2))/3) \quad (1)$$

where **V** is the volume
L is the distance between the cross sections
$\mathbf{S_1}$ is the area of one end of the frustum, and
$\mathbf{S_2}$ is the area of the other end of the frustum.

Substituting values from table 7D–4 into the formula results in:

$$967{,}176 = 202* ((1{,}800 + 8{,}625 + sqrt\ (1{,}800*8{,}625)) /3) \quad (2)$$

if the fractions are rounded to the nearest whole number after each intermediate calculation. Multiplying the volumetric weight (specific gravity) of the mineralized material (in this case, 3.91 t/m^3, the mean specific gravity of samples collected in mineralized block 3A, from table 7D–4A) by the volume of 967,176 m^3 results in a tonnage of about 3,782,000 t for block 3A. The percent iron and percent sulfur values in table 7D–4A are averaged from geochemical samples in trenches and drill holes in the specific mineralized blocks.

The remainder of the A, B, C_1, and C_2 resources are calculated the same way. The only difference is the formula used to calculate the volumes of the various geometric shapes that represent the various mineral blocks.

7D.2.2.4 Prognosis Resources

As shown above, fully explored and evaluated resource categories are based on sampling and exploration. In contrast, prognosis resources are unsampled and crudely estimated. Table 7D–5 shows the amounts of prognosis resources estimated for the Haji-Gak iron deposit and the data used to calculate those resources (Kusov and others, 1965b). As can be seen in the table, the lengths and widths are rounded to the nearest 5 or 10 m, although the down-dip thickness is measured to the nearest 0.1 m; the specific gravity is a constant 4.01 t/cubic meters estimated from similar samples collected in the better explored western part of the deposit, and the volumetric calculations are based on the formula for finding the volume of a rectangular prism:

$$V= L \times W \times T$$

where **V** is the volume,
L is the length of the mineralized block,
W is the width of the mineralized block, and
T is the down-dip thickness of the mineralized block.

The resultant volume in m^3 is multiplied by the specific gravity to determine the tonnage of mineralized resources in the each block. Totaling the estimates of prognosis material listed in table 7D–5 shows that the mineralized blocks are suspected of containing 332,674,125 m^3 or 1,334,023,242 t of iron-mineralized rock. While the assessment methods of the 1960s for determining the amount of prognosis resources may seem crude by today's standards, the geologists were on the ground evaluating a deposit that in large part they could see and touch, so their resource estimates, no matter how unsophisticated, are based on the science of the times.

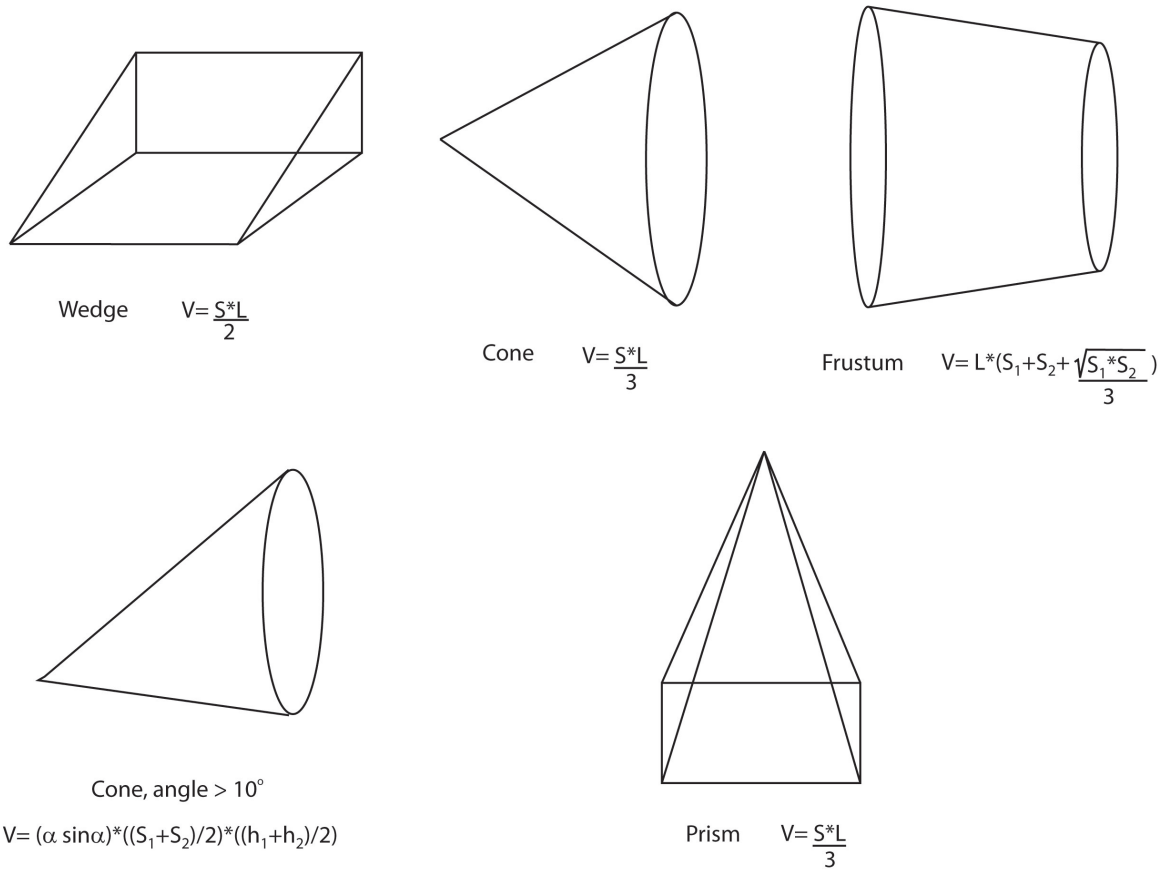

Figure 7D–12. Examples of solid geometrical figures and formulas for calculating their volumes (after Kusov and others, 1965b; and Popoff, 1966). Such figures were used to represent resource blocks to estimate iron resources.

7D.22.5 Fragmental Resources

Fragmental iron resources are widely developed at Haji-Gak (figures7D–1, 7D–2, and 7D–4 through 7D–7). They form thin surficial alluvial-talus deposits over a considerable area generally at the base of the exposed iron deposits and spread away from the in-situ mineralization as much as 1.5 km (Kusov and others, 1965b). They are completely exposed or are covered with a sandy soil as much as 1.5 m thick. The deposits are made up of mostly iron-rich boulders from 0.5 to 2.5 m in diameter and averaging 61.67 percent Fe, which differs little from the in-situ material (Kusov and others, 1965b). Some fragments of mineralized rock are also included. The boulders may consist of hydrogoethite-half

martite, hydrogoethite-hematite-half martite, and rarely carbonate-half martite mineralization. Four deposits of fragmental resources were identified by Kusov and others (1965b), and three of the four were evaluated for prognosis iron resources (table 7D–6). At 100,000 m^2 and 470,532 t, fragmental deposit A was considered too small to be a resource (Kusov and others, 1965b). The three evaluated deposits of fragmental iron-bearing rock are estimated to contain a total of 16,549,749 m^3 or 11,220,730 t of material.

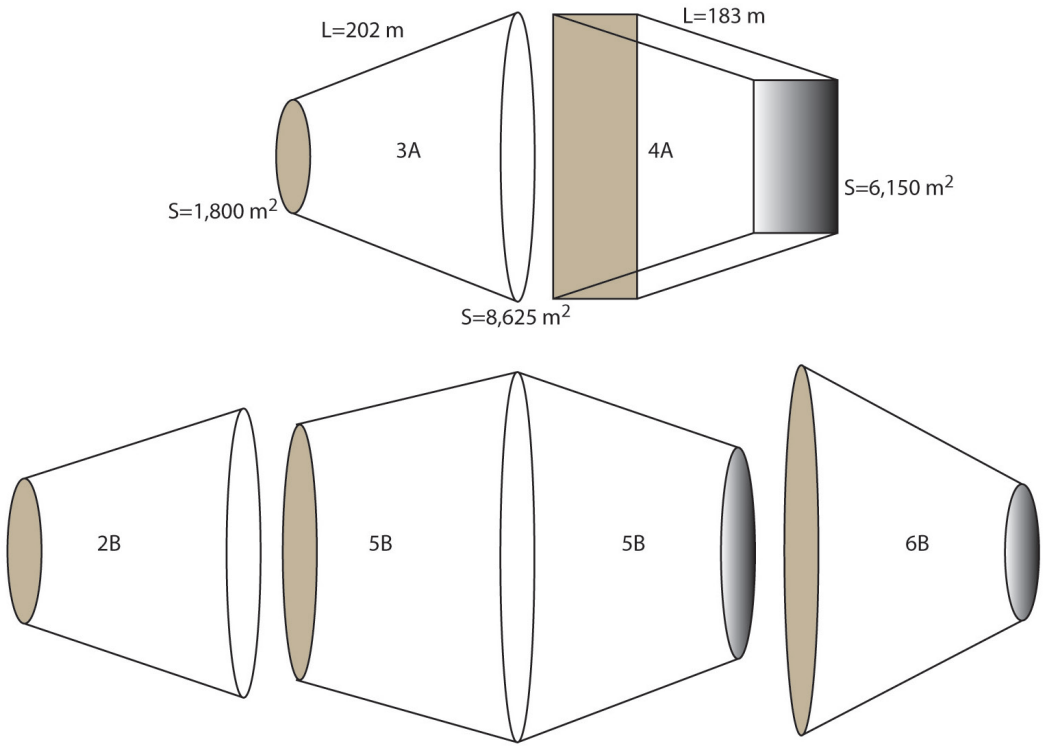

Figure 7D–13. Resources categories A and B in mineralized body 1 of the Haji-Gak iron deposit as represented by solid geometrical figures used in calculating the volume of resources. The figures used are described in Kusov and others (1965b); not to scale. Resource blocks 2B, 3A, 4A, 5B, and 6B occur in the better explored part of mineralized body 1.

Table 7D–4A. Estimated iron resources by resource block and mineralized body with the dimensions, the solid geometrical shapes used in the resource calculations, and the formulas used to calculate the volumes.

[Modified from Kusov and others (1965b). The possibly excessive number of significant figures for volumes and resources is in the original tables of Kusov and others (1965b)]

Mineralized block	Resource category	Cross-section number	Number of 5 m × 5 m squares within area	Area of mineralized body (m^2) (S)	Distance between cross sections in m (L)	Block volume (m^3)	Specific gravity (t/m^3)	Tonnage (1,000 t)	Iron (percent)	Sulfur (percent)	Geometric figure used	Formula	Mineralized material
3	A	3	72	1,800	202	967,176	3.91	3,782	63.13	0.15	Frustum	$V=L*((S_1+S_2)+sqrt(S_1*S_2)/3)$	Hydrogoethite-semimartite
		4	345	8,625									
4	A	4	345	8,625	183	1,351,821	3.91	5,286	61.91	0.13	Mean-area	$V=L*((S_1+S_2)/2)$	Hydrogoethite-semimartite
		5	25	6,150									
Total A			345	8,625				9,068	62.52	0.14			
2	B	2	58	1,450	214	938,818	3.91	3,671	64.32	0.07	Frustum	$V=L*((S_1+S_2)+sqrt(S_1*S_2)/3)$	Hydrogoethite-semimartite
		3	330	8,250									
5	B	3	258	6,450	204	1,683,000	3.91	6,580	64.13	0.15	Frustum	$V=L*((S_1+S_2)+sqrt(S_1*S_2)/3)$	Hydrogoethite-semimartite
		4	408	10,200									
		4	408	10,200									
		5	165	4,125	186	1,434,060	3.91	5,607	61.94	0.16	Frustum	$V=L*((S_1+S_2)+sqrt(S_1*S_2)/3)$	Hydrogoethite-semimartite
6	B	5	411	10,275	284	866,200	3.91	3,387	61.11	0.09	Frustum	$V=L*((S_1+S_2)+sqrt(S_1*S_2)/3)$	Hydrogoethite-semimartite
		6	53	1,325									
Total B								19,245	–	–			
Total A+B								28,313	–	–			
1	C_1	1	22	550	496	3,248,992	3.91	12,704	64.20	0.07	Angle greater than 10^o ($a=34^o$)	$V=(\alpha/\sin\alpha)*((S_1+S_2)/2)*((h_1+h_2)/3)$	Hydrogoethite-semimartite
		2	624	15,600									
Total of $1C_1$								12,704					
7	C_1	2	566	14,150	225	1,805,917.5	3.91	7,061	64.90	0.07	Frustum	$V=L*((S_1+S_2)+sqrt(S_1*S_2)/3)$	Hydrogoethite-semimartite
		3	128	3,200									

Mineralized block	Resource category	Cross-section number	Number of 5 m × 5 m squares within area	Area of mineralized body (m^2) (S)	Distance between cross sections in m (L)	Block volume (m^3)	Specific gravity (t/m^3)	Tonnage (1,000 t)	Iron (percent)	Sulfur (percent)	Geometric figure used	Formula	Mineralized material
	$C_{1(a)}$	3	128	3,200	205	514,058	3.91	2,010	64.70	0.15	Frustum	$V=L*((S_1+S_2)+sqrt(S_1*S_2)/3)$	Hydrogoethite-semimartite
		4	128	1,875									
		4	128	1,875	194	240,598.8	3.91	941	61.68	0.17	Frustum	$V=L*((S_1+S_2)+sqrt(S_1*S_2)/3)$	Hydrogoethite-semimartite
		5	28	700									
Total of $7C_1+C_{1(a)}$								10,012	63.28	0.12			
7	$C_{1(b)}$	–	0	0									
		4	206	5,150	140	360,500	4.12	1,485	59.27	4.29	Wedge	V= (S*L)/2	Pyrite-magnetite ore
		4	206	5,150	194	652,226.8	4.12	2,687	59.27	4.29	Frustum	$V=L*((S_1+S_2)+sqrt(S_1*S_2)/3)$	Pyrite-magnetite ore
		5	74	1,850									
Total of $7C_{1(b)}$								4,172	59.27	4.29			
8	$C_{1(a)}$	5	28	700	264	1,169,440.8	3.91	4,573	59.27	4.29	Frustum	$V=L*((S_1+S_2)+sqrt(S_1*S_2)/3)$	Hydrogoethite-semimartite
		6	398	9,950									
		6	450	11,250	368	4,686,066	3.91	18,323	68.83	0.1	Angle greater than 10^o ($a=16^o$)	$V=(\alpha/\sin\alpha)*((S_1+S_2)/2)*((h_1+h_2)/2)$	Hydrogoethite-semimartite
		7	579	14,475									
Total of $8C_{1(a)}$								22,896	–	–			
8	$C_{1(a)}$	5	74	1,850	264	778,800	4.12	3,209	59.27	4.29	Angle greater than 10^o ($a=18^o$)	V=(a/sina)* (S1+S2)/2*L	Pyrite-magnetite ore
		6	162	4,050									
	$C_{1(b)}$	6	162	4,050									
		7	74	4,125	368	1,489,158	4.12	6,135	59.27	4.29	Mean-area	V=L*(S1+S2)/2)	Pyrite-magnetite ore
Total of $8C_{1(a)} + C_{1(b)}$								9,344	59.27	4.29			

Mineralized block	Resource category	Cross-section number	Number of 5 m × 5 m squares within area	Area of mineralized body (m^2) (S)	Distance between cross sections in m (L)	Block volume (m^3)	Specific gravity (t/m^3)	Tonnage (1,000 t)	Iron (percent)	Sulfur (percent)	Geometric figure used	Formula	Mineralized material
9	$C_{1(a)}$	7	579	14,475	300	2,171,250	3.91	8,490	61.26	–	Wedge	V= (S*L)/2	Hydrogoethite-semimartite
		8	0	0									
	$C_{1(b)}$	7	165	4,125	150	309,375	4.12	1,275	59.27	4.29	Wedge	V= (S*L)/2	Pyrite-magnetite ore
		–	0	0									
Total $9C_{1(a)} + C_{1(b)}$								9,765	–	–			
Total C_1								68,893	–	–			
10	C_2	–	0	0	246	735,950	3.91	2,878	63.87	–	Cone	V= (S*L)/3	Hydrogoethite-semimartite and carbonate-semimartite ores
		1	359	8,975									
11	C_2	1	337	8,425	437	3,803,429.5	4.01	15,252	64.20	0.07	Angle greater than 10^0 ($a=34^0$)	$V=(\alpha/\sin\alpha)*((S_1+S_2)/2)*((h_1+h_2)/2)$	Hydrogoethite-semimartite and pyrite-magnetite ore
		2	339	8,475									
		2	339	8,475	233	1,097,033.9	4.01	4,399	61.90	2.18	Frustum	$V=L*((S_1+S_2)+sqrt(S_1*S_2)/3)$	Hydrogoethite-semimartite and pyrite-magnetite ore
		3	71	1,775									
		3	71	1,775	200	646,000	4.12	2,662	59.27	4.29	Frustum	$V=L*((S_1+S_2)+sqrt(S_1*S_2)/3)$	Pyrite-magnetite ore
		4	198	4,950									
		4	198	4,950	199	545,916.7	4.12	2,249	59.27	4.29	Frustum	$V=L*((S_1+S_2)+sqrt(S_1*S_2)/3)$	Pyrite-magnetite ore
		5	41	1,025									
		5	41	1,025	259	135,327.5	4.12	558	59.27	4.29	Frustum	$V=L*((S_1+S_2)+sqrt(S_1*S_2)/3)$	Pyrite-magnetite ore
		6	6	150									
		6	6	150	325	112,612.5	4.12	464	59.27	4.29	Angle greater than 10^o	$V=(\alpha/\sin\alpha)*((S_1+S_2)/2)*((h_1+h_2)/2)$	Pyrite-magnetite ore
		7	24	600									

Mineralized block	Resource category	Cross-section number	Number of 5 m × 5 m squares within area	Area of mineralized body (m^2) (S)	Distance between cross sections in m (L)	Block volume (m^3)	Specific gravity (t/m^3)	Tonnage (1,000 t)	Iron (percent)	Sulfur (percent)	Geometric figure used	Formula	Mineralized material
		7	24	600	300	372,690	4.01	1,494	61.57	2.17	Frustum	V=L*((S1+S2)+sqrt(S1*S2)/3)	Hydrogoethite-semimartite and pyrite-magnetite ore
		8	81	2,025									
12	C_2	8	81	2,025	106	107,325	3.91	420	63.88	0.06	Wedge	V= (S*L)/2	Hydrogoethite-semimartite ore
		–	0	0									
Total C_2								30,376	61.08	3.08			

Table 7D–4B. Estimated iron resources in mineralized body 2 by resource block with the dimensions, the solid geometrical shapes used in the resource calculations, and the formulas used to calculate the volumes.

[Modified from Kusov and others (1965b). The possibly excessive number of significant figures for volumes and resources is in the original tables of Kusov and others (1965b)]

Mineralized block	Resource category	Cross-section number	Number of 5 m x 5 m squares within area	Area of mineralized body (m^2)	Distance between cross sections in m (L)	Block volume (m^3)	Specific gravity (t/m^3)	Tonnage (1,000 t)	Iron (percent)	Sulfur (percent)	Geometric figure used	Formula	Mineralized material
13	$C_{1(a)}$	4	24	600	199	144,275	3.91	564	62.86	0.10	Mean-Area	V=L*((S1+S2)/2)	Hydrogoethite-semimartite ore
		5	34	850									
13	$C_{1(a)}$	5	34	850	254	180,975	3.91	708	62.36	0.10	Mean-Area	V=L*((S1+S2)/2)	Hydrogoethite-semimartite ore
		6	23	575									
13	$C_{1(a)}$	6	23	575	327	1,181,161.2	3.91	4,618	61.44	0.19	Angle greater than 10^o	(α/sinα)*((S1+S2)/2)*((h1+h2)/2)	Hydrogoethite-semimartite ore
		7	328	8,200									
Total 13$C_{1(a)}$								5,890	62.22	0.16			
13	$C_{1(b)}$	–	0	0	180	121,500	4.12	501	63.33	4.83	Wedge	V= (S*L)/2	Pyrite-magnetite ore
		7	54	1,350									

Mineralized block	Resource category	Cross-section number	Number of 5 m x 5 m squares within area	Area of mineralized body (m^2)	Distance between cross sections in m (L)	Block volume (m^3)	Specific gravity (t/m^3)	Tonnage (1,000 t)	Iron (percent)	Sulfur (percent)	Geometric figure used	Formula	Mineralized material
Total 13 $C_{1(a)}$, $C_{1(b)}$								6,391	–	–			
14	$C_{1(a)}$	–	0	0	316	1,295,600	3.91	5,066	62.44	0.29	Wedge	V= (S*L)/2	Hydrogoethite-semimartite ore
		7	328	8,200									
14	$C_{1(b)}$	–	0	0	316	213,300	4.12	879	63.33	4.83	Wedge	V= (S*L)/2	Pyrite-magnetite ore
		7	54	1,350									
Total 14 $C_{1(a)}$+ $C_{1(b)}$								5,945	–	–			
Total C_1								12,336	–	–			
15	C_2	–	0	0	38	3,166.6	4.01	13	–	–	Cone	V= (S*L)/3	Hydrogoethite-semimartite and pyrite-magnetite ores
		1	10	250									
16	C_2	1	10	250	359	2,022,752.83	4.01	8,111	60.98	0.07	Angle greater than 10^o ($\alpha=34^o$)	$(\alpha/\sin\alpha)*((S_1+S_2)/2)*((h_1+h_2)/2)$	Hydrogoethite-semimartite and pyrite-magnetite ores
		2	571	14,275									
16	C_2	2	571	14,275	303	3,345,604.8	4.01	13,416	61.97	0.07	Frustum	$V=L*((S_1+S_2)+\text{sqrt}(S_1*S_2)/3)$	Hydrogoethite-semimartite and pyrite-magnetite ores
		3	324	8,100									
16	C_2	3	324	8,100	198	1,732,500	4.01	6,947	61.83	0.04	Mean-Area	$V=L*((S_1+S_2)/2)$	Hydrogoethite-semimartite and pyrite-magnetite ores
		4	376	9,400									

Mineralized block	Resource category	Cross-section number	Number of 5 m x 5 m squares within area	Area of mineralized body (m^2)	Distance between cross sections in m (L)	Block volume (m^3)	Specific gravity (t/m^3)	Tonnage (1,000 t)	Iron (percent)	Sulfur (percent)	Geometric figure used	Formula	Mineralized material
Total $15C_2$ + $16C_2$								28,487	61.55	0.06			
17	C_2	4	352	8,800	206	999,512	4.01	4,008	62.28	0.04	Frustum	$V=L*((S_1+S_2)+sqrt(S_1*S_2)/3)$	Hydrogoethite-semimartite and pyrite-magnetite ores
		5	156	3,900									
17	C_2	5	156	3,900	250	347,900	4.01	1,395	62.36	0.10	Frustum	$V=L*((S_1+S_2)+sqrt(S_1*S_2)/3)$	Hydrogoethite-semimartite and pyrite-magnetite ores
		6	0.68	17									
17	C_2	6	0.68	17	325	544,417.25	4.01	2,183	62.09	2.46	Angle greater than 10^o ($\alpha=18^o$)	$(\alpha/sin\alpha)*((S_1+S_2)/2)*((h_1+h_2)/2)$	Hydrogoethite-semimartite and pyrite-magnetite ores
		7	189	4,725									
Total $17C_2$								7,586	62.18	1.65			
18	C_2	7	189	4,725	324	2,476,980	4.01	9,933	63.74	2.45	Frustum	$V=L*((S_1+S_2)+sqrt(S_1*S_2)/3)$	Hydrogoethite-semimartite and pyrite-magnetite ores
		8	440	11,000									
19	C_2	–	0	0	64	352,000	4.01	1,412	64.16	0.07	Wedge	$V= (S*L)/2$	Hydrogoethite-semimartite and pyrite-magnetite ores
		8	440	11,000									
Total $18C_2$ + $19C_2$								11,345	–	–			
Total C_2								47,418	–	–			

Mineralized block	Resource category	Cross-section number	Number of 5 m x 5 m squares within area	Area of mineralized body (m^2)	Distance between cross sections in m (L)	Block volume (m^3)	Specific gravity (t/m^3)	Tonnage (1,000 t)	Iron (percent)	Sulfur (percent)	Geometric figure used	Formula	Mineralized material

Table 7D–4C. Estimated iron resources in mineralized body 9 by resource block with the dimensions, the solid geometrical shapes used in the resource calculations, and the formulas used to calculate the volumes.

[Modified from Kusov and others (1965b). The possibly excessive number of significant figures for volumes and resources is in the original tables of Kusov and others (1965b)]

Mineralized block	Resource category	Trench stripping 7, 8 and 8a	Number of 5 m x 5 m squares within area	Area of mineralized body (m^2)	Distance between cross sections in m (L)	Block volume (m^3)	Specific gravity (t/m^3)	Tonnage (1,000 t)	Iron (percent)	Sulfur (percent)	Geometric figure used	Formula	Mineralized material
20	C_2	7	1,800	45,000	470	10,575,000	4.01	42,406	63.42	0.12	Wedge	$V= (S*L)/2$	Hydrogoethite-semimartite and pyrite-magnetite ores
		–	0	0									
21	C_2	7	1,800	45,000	1060	41,320,125	4.01	165,694	62.18	0.08	Angle greater than 10° (α=21°)	$V=(\alpha/\sin\alpha)*((S_1+S_2)/2)*((h_1+h_2)/2)$	Hydrogoethite-semimartite and pyrite-magnetite ores
		8-8a	150	3,750									
22	C_2	8	750	18,750	410	3,843,750	4.01	15,413	62.06	0.06	Wedge	$V= (S*L)/2$	Hydrogoethite-semimartite and pyrite-magnetite ores
		–	0	0									
		–	0	0									
23	C_2	8a	600	15,000	430	3,225,000	4.01	12,932	61.08	0.07	Wedge	$V= (S*L)/2$	Hydrogoethite-semimartite and pyrite-magnetite ores
Total C_2								236,445	62.18	0.08			

Table 7D–5. Estimated P2 (prognosis) resources by mineralized body.

[Data are from Kusov and others (1965b). Specific gravity was estimated from similar samples collected in the better explored western part of the deposit. The possibly excessive number of significant figures for volumes and resources is in the original tables of Kusov and others (1965b)]

Mineralized body	Length (m)	Width (m)	Down-dip thickness (m)	Volume (m^3)	Specific gravity (t/m^3)	Resources (t)
1	2,200	370	46.5	37,851,000	4.01	151,782,510
2	240	150	35.2	1,267,200	4.01	5,081,472
3	800	105	9.7	814,800	4.01	3,267,348
4	290	55	22.6	360,470	4.01	1,445,485
5	60	20	7	8,400	4.01	33,684
6	315	150	21.3	1,006,425	4.01	4,035,764
7	210	75	11.4	179,550	4.01	719,996
7a	150	50	11.2	84,000	4.01	336,840
8	650	200	24.7	3,211,000	4.01	12,876,110
9	3,360	350	133.2	156,643,200	4.01	628,139,232
10	550	190	24.2	2,528,900	4.01	10,140,889
11	840	200	54.1	9,088,800	4.01	36,446,088
12	1,600	510	141.1	115,137,600	4.01	461,701,776
13	260	120	14.3	446,160	4.01	1,789,102
14	480	170	45.9	3,745,440	4.01	15,019,214
15	220	55	10.8	130,680	4.01	524,027
16	250	55	12.4	170,500	4.01	683,705
Totals	–	–	–	332,674,125	–	1,334,023,242

Table 7D–6. Estimated iron resources by fragmental deposit with the estimated thicknesses and areas.

[Specific gravity is the mass of the iron-bearing mineralized rock per cubic meter of fragmental deposit. Estimated thickness is an average for the fragmental deposits based on several measurements.]

Deposit	Estimated thickness	Area (m2)	Volume (m3)	Specific gravity (t/m^3)	Resource (t)
B	6.94	859,690	5,966,249	0.678	4,045,117
C	6.94	750,000	5,205,000	0.678	3,528,990
D	6.94	775,000	5,378,500	0.678	3,646,623
Totals	–	2,384,690	16,549,749	–	11,220,730

7D.3 Conclusions

The Haji-Gak iron deposit is the best explored and well exposed iron deposit along the 600-km-long trend of mineralization in central Afghanistan, but the fully explored and evaluated resources of the deposit are but a small part of the total deposit. In the early 1960s, geologists from the Soviet Union and the Royal Afghan Government mapped and sampled the Haji-Gak iron deposit and estimated its resources in several categories including prognosis resources. The fully explored (A, B, and C_1) resources amount to 110.8 million metric tons (Mt), or about 6 percent of the deposit, while the evaluated (C_2) and prognosis (P_2) resources make up about 94 percent of the almost 1,800 Mt of estimated resources. The estimates of prognosis resources have been become entrenched in the literature.

This report examines the previous resource estimates by recreating the calculations made in the early 1960s using the maps, cross sections, and data tables in Kusov and others (1965b). The estimates of the categories A, B, and C_1 resources, amounting to 110.8 Mt, were found to be supported by observations made in the field, based on logical conclusions, and scientifically credible for the technology of the era. At current market conditions, the potential profit in 110.8 Mt of iron ore may not compare favorably to

the costs of mine and infrastructure development. The C_2 (based on a loose exploration grid with little data) and P_2, (prognosis) resources, however, are based on field estimations of the size of the mineralized bodies. Estimations of the possible iron grades of those bodies are based on observations from the better explored bodies, because the mineralized rocks were buried beyond the reach of the drill holes and shafts or were in bodies that were not explored. Further exploration has the potential to upgrade current C_2 and P_2 resources to A, B, and C_1 resources and enhance the potential for iron mining at Haji-Gak. Much more exploration, sampling, and analysis is needed before an economic evaluation of the deposit can be made.

7D.4 Acknowledgments

The authors would like to thank Bill Cannon, Avery Drake, Dan Hayba, Dave Menzie, and Klaus Schulz of the U.S. Geological Survey for their help and thoughtful review comments that greatly improved the manuscript.

7D.5 References Cited

Abdullah, Sh., Chmyriov, V.M., Stazhilo-Alekseev, K.F., Dronov, V.I., Gannan, P.J., Rossovskiy, L.N., Kafarskiy, A.Kh., and Malyarov, E.P., 1977, Mineral resources of Afghanistan (2d ed.): Kabul, Afghanistan, Republic of Afghanistan Geological and Mineral Survey, 419 p.

Afghanistan Geological and Mineral Survey, 1967, Geological structure of the Haji Gak iron deposit and its commercial value: Afghanistan Geological and Mineral Survey, Kabul, 13 p.

Afghanistan Geological Survey, undated, Minerals in Afghanistan—The Hajigak iron deposit: Secretariat for the Ministry of Mines, Kabul, Afghanistan, in cooperation with the British Geological Survey, 6 p., available at http://www.bgs.ac.uk/afghanminerals/femetals.htm. Accessed June 29, 2011.

Afghanistan Ministry of Mines, 2011, Hajigak iron deposit: Islamic Republic of Afghanistan, available at http://ww http://mom.gov.af/en/page/1382. Accessed June 29, 2011.

Afzali, H., 1981, Les ressources d'hydrocarbures, de métaux e de substances utiles de l'Afghanistan: aperçu général: Chronique de la Recherche Minière, no. 460, p. 29–51.

Bouladon, Jean, and de Lapparent, A.F., 1975, Le minerai de fer d'Hajigak (Afghanistan). Position stratigraphique, cadre géologique et type du gisement: Mineralium Deposita, v. 10, p. 13–25.

Brueckl, K., 1935, Mineral deposits of eastern Afghanistan, unpub. data.

Chmyriov, V.M., Stazhilo-Alekseev, K.F., Mirzad, S.H., Dronov, V.I., Kazikhani, A.R., Salah, A.S., and Teleshev, G.I., 1973, Mineral resources of Afghanistan, in Geology and mineral resources of Afghanistan: Kabul, Afghanistan Department of Geological Survey, p. 44–85.

Cox, D.P., Barton, P.B., and Singer, D.A., 1986, Introduction, *in* Cox, D.P., and Singer, D.A., eds., Mineral deposit models: U.S. Geological Survey Bulletin 1693, p. 1–10.

DEMAG (Creusot-Loire enterprises), 1974, Feasibility study for an integrated iron and steel plant in Afghanistan, Duisberg, Germany, April, DEMAG, .

de Lapparent, A.F., 1961, Un gisement de minerai de fer en Afghanistan central [Deposits of iron in Central Afghanistan]: C.R. Academy of Science, v. 253, p. 2556.

Henley, Stephen, 2000, The Russian system of resource/reserves classification: Earth Science Computer Applications, v.15, no. 12, p.1–2.

Henley, Stephen, 2004, The Russian reserves and resources reporting system—Discussion and comparison with international standards: Resources Computing International Ltd., 13 p., available at http://www.imcinvest.com/pdf/Russian_reserves_8.pdf. Accessed June 29, 2011.

InfoMine, 2011, Hajigak Iron deposit—Request for expression of interest, Hajigak iron: Available at http://www.infomine.com/properties/exchange/listings/2016/property.aspx. Accessed June 29, 2011.

Kusov, I.K., Smirnov, M.S., and Reshetayak, V.V., 1965a, Report on prospecting and survey at iron occurrences in Central Afghanistan and the Hajigak iron deposit's estimated reserves: Department of Geological and Mineral Survey, Kabul, unpub. data.

Kusov, I.K., Smirnov, M.S., and Reshetayak, V.V., 1965b, Report on the results of prospecting-survey and reconnaissance works for iron ores in Central Afghanistan with reserve calculation on Hajigak deposit for 1963–1964: USSR v/o Technoexport, contract no. 640, 3 volumes with English translation, Kabul, unpub. data.

Kužvart, M.S., and Böhmer, Miloslav, 1978, Prospecting and exploration of mineral deposits, in Developments in economic geology, v. 8: Oxford, New York, Elsevier Scientific Publishing Co., 431 p.

Mining Weekly, 2011, Afghanistan invites bids for Hajigak iron deposit: Mining Weekly, available at http://www.miningweekly.com/article/afghanistan-invites-bids-for-hajigak-iron-deposit-2011-01-19. Accessed February, 2011.

Momji, G.S., and Chaikin, S.I., 1960, Iron ores of Afghanistan: Kabul, DGMS.

Orris, G.J., and Bliss, J.D., 2002, Mines and mineral occurrences of Afghanistan: U.S. Geological Survey Open-File Report 02–110, 95 p.

Peters, S.G., 2007, Sedimentary rock-hosted iron deposits, in Peters, S.G., Ludington, S.D., Orris, G.J., Sutphin, D.M., Bliss, J.D., and Rytuba, J.J., eds., and the U.S. Geological Survey-Afghanistan Ministry of Mines Joint Mineral Resource Assessment Team, Preliminary non-fuel mineral resource assessment of Afghanistan: U.S. Geological Survey Open-File Report 2007–1214 (Afghanistan Geological Survey Open-File Report 2007–1214) p. 344–365.

Peters, S.G., Ludington, S.D., Orris, G.J., Sutphin, D.M., Bliss, J.D., and Rytuba, J.J., eds., and the U.S. Geological Survey-Afghanistan Ministry of Mines Joint Mineral Resource Assessment Team, 2007, Preliminary non-fuel mineral resource assessment of Afghanistan: U.S. Geological Survey Open-File Report 2007–1214 (Afghanistan Geological Survey Open-File Report 2007–1214), 852 p.

Popoff, C.C., 1966, Computing reserves of mineral deposits—Principles and conventional methods: U.S. Bureau of Mines Information Circular 8283, 113 p.

Renaud, K.M., Tucker, R.D., Peters, S.G., Stettner, W.R., Masonic, L.M., and Moran, T.W., comps., 2011a, Geologic map of the Haji-Gak iron deposit, Bamyan Province, Afghanistan, modified from the 1965 original map compilation of M.S. Smirnov and I.K. Kusov: U.S. Geological Survey Open-File Report 2011–1185–A, one sheet, scale 1:10,000, available at *http://pubs.usgs.gov/of/2011/1185/A/*.

Renaud, K.M., Tucker, R.D., Peters, S.G., Stettner, W.R., Masonic, L.M., and Moran, T.W., comps., 2011b, Geologic map of the western Haji-Gak iron deposit, Bamyan Province, Afghanistan, modified from the 1965 original map compilation of V.V. Reshetniak and I.K. Kusov: U.S. Geological Survey Open-File Report 2011–1185–B, one sheet, scale 1:4,000, available at *http://pubs.usgs.gov/of/2011/1185/B/*.

Robinson, Matt, and Shalizi, Hamid, 2011, Afghanistan invites bids for Hajigak iron deposit: Reuters, January 19, 2011, available at http://uk.reuters.com/article/2011/01/19/afghanistan-hajigak-idUKSGE70I0BB20110119. Accessed June 29, 2011.

Thrush, P.W., and the Staff of the Bureau of Mines, comp. and eds, 1968, A dictionary of mining, mineral, and related terms: U.S. Bureau of Mines, 1269 p.

United Nations Economic and Social Commission for Asia and the Pacific (ESCAP), 1995, Geology and mineral resources of Afghanistan: United Nations Economic and Social Commission for Asia and the Pacific Atlas of Mineral Resources of the ESCAP Region, v. 12, 85 p.

U.S. Departments of State and Defense, cohosts, 2011, Towards a New Silk Road Conference: NESA Center and State Department, June 7–8, 88 p.

Venot-Pic, 1974, Feasibility study relating to the development of the Hajigak iron ore mine and Shabashak coal mine: Paris, France, Venot-Pic, [unpaginated].